



## Immune Network at the Edge of Chaos

AMÉRICO T. BERNARDES\*‡ AND RITA M. ZORZENON DOS SANTOS†

\**Institute for Theoretical Physics, Cologne University, D-50923 Cologne, Germany*; †*Instituto de Física—Universidade Federal Fluminense, Av. Litorânea, s/n-Boa Viagem, 24210-340, Niterói-RJ, Brazil*

(Received on 30 May 1996, Accepted on 27 November 1996)

Some time ago Jerne proposed a new theory to explain the basis of the behaviour of the immune system. He suggested the existence of a functional connected network, based on pattern recognition of the idiotypes carried by the lymphocytes, which is responsible for the self regulation of the immune system. Only 15–20% of the lymphocytes available in the immune repertoire will participate in this functional network, while the rest of the lymphocytes will be free to respond to any foreign antigen. Each individual immune repertoire will be different depending on the lymphocytes that participate in the connected network.

Using a very simple cellular automata model of the immune repertoire dynamics we show that, although the usual regimes (stable and chaotic) attained by this automata, are not interesting from the biological point of view, the transition region, at the edge of chaos, is very appropriate to describe such dynamics. In this region we have obtained a functional connected network involving 10–20% of the lymphocytes available in the repertoire, as suggested by Jerne and others. The model also reproduces the immune system signature, the ensemble of different lymphocytes that each individual expresses in his immune repertoire, which varies from one individual to another. We show how the immune memory comes out as a consequence of the dynamics of the system. From our results we confirm and present evidence that the chaotic regime corresponds to a sort of non-healthy state, as has been suggested previously.

© 1997 Academic Press Limited

### 1. Introduction

Twenty years ago, Niels Jerne (Jerne, 1974) introduced the basic concepts of a new vision of the immune system. In his proposal, the immune system is regulated by a functional complex network defined by the idiotype/anti-idiotype interactions.

The antigen carries unique antigenic determinants, called *epitopes*. Epitopes are patches on the antigen molecule, which exhibit a pattern that can be recognized with a good precision by complementary patterns of the *paratopes*, which are the specific combining sites carried by the antigen specific antibodies. The paratope of the cell receptor has the

same molecular structure of the antibodies that will be secreted by those cells. Epitopes and paratopes enable the immune system to accomplish its task of pattern recognition. As experimentally demonstrated, the antibody molecules also present epitopes that can play a functional role. The set of epitopes displayed by the variable regions of a set of antibody molecules is called *idiotype*, and each single idiotypic epitope is denominated *idiotope*. Collectively, the idiotopes on each antibody can be interpreted as written letters, and the idiotype of this antibody as its own signature. For simplicity we can assume that the repertoires of paratopes and idiotopes are of the same order of magnitude. The antibodies can recognize their complementary molecular structure via paratopes and can also be recognized via idiotopes. The recognition of the antibody molecules by other

†Author to whom correspondence should be addressed.

‡Present and permanent address: Departamento de Física, Universidade Federal de Ouro Preto, 35400-000. Ouro Preto-Mg, Brazil.

antibody molecules in the same serum can be conceived as a huge and complex network of paratopes that recognize sets of idiotopes, and idiotopes that are recognized by sets of paratopes. The idiotopes presented on the antibodies produced in the first wave of an immune response can then behave as antigens to trigger a second response. The second-wave of antibodies will be directed against the idiotypes of the first-wave antibodies, the second-wave population is generally referred to as anti-idiotypic antibodies. These, in turn, can induce a third wave of antibodies and so on. The recognition of the antigen (epitope) by the paratope of the cell can lead to a positive response, which generates cell proliferation, cell activation and antibody secretion, or to a negative one that results in tolerance or suppression. The Jerne theory assumes that the dynamics of activation and suppression of the functionally connected network is the key factor of the self regulation of the immune system. The immune system achieves a dynamic state in which its elements interact among themselves, in such a way that some populations decay and new ones grow, thus the activation does not propagate indefinitely, in the sense that there is no percolation of the information. According to such a view, the immune memory is a consequence of network interactions, in contrast with some theories which claim that the immune memory is due to the persistence of long-lived memory cells (Jerne, 1974; Schitteck & Rajewsky, 1990).

The hypothesis of a permanent dynamical behaviour of the immune system, is confirmed by the observation that the fluctuations of idiotypes in serum concentration were found to follow chaotic or oscillatory regimes (Holmberg *et al.*, 1989). A large amount of experimental evidence of idiotope-anti-idiotope interactions has been obtained, as for instance in the recent work of Evans *et al.* (1994) in which they determine the anti-idiotope (internal image) that mimics the brucellosis antigen. Although the original proposal of the network theory was concerned with B-cells and antibodies, experiments showed that T-cells also interact through idiotope specificities (Johnson-Léger & Dean, 1994).

Considering the available experimental evidence, several questions must be answered. One important point is that there is no clear evidence of a fully connected network. As pointed out by Coutinho (1989) and Holmberg *et al.* (1989), the majority of the lymphocytes (B or T) are small resting cells ( $\sim 80\%$ ). Thus, the activated cells would form compartments, disconnected at least in time, as stated by Holmberg *et al.* (1989). Since some of the mechanisms of self-regulation are still not clear, there are some

questions that we may ask (if one adheres to the idea of a fully connected network): once the immune system exhibits an activation chain, as explained above, what prevents the immune response from continuing to expand in successive waves until the entire system is involved? Is it true that the dynamics of the connected network supported by the stimulation and suppression mechanisms is responsible for the self-regulation of the immune repertoire?

Since the introduction of the network hypothesis, several different models with many different mathematical approaches have been developed, with the aim of reproducing the basic aspects of the theory (see for example Perelson, 1988, 1992; Weisbuch *et al.*, 1990, 1993; Neumann & Weisbuch, 1992; Stewart & Varela, 1991; Sulzer *et al.*, 1994; and Monvel & Martin, 1995). In this paper we consider a simple cellular automata model proposed by Stauffer & Weisbuch (1992) based on a previous one introduced by De Boer and co-workers (1992) to describe the dynamic evolution of the immune repertoire. Those models refer only to B-cell response and are based on the idea of complementary shapes (lock-and-key) used to describe the recognition of the idiotope/anti-idiotope populations that would correspond to the recognition of the antigen by the lymphocytes and/or antibodies or even antibodies/anti-antibodies. The automaton rule depends on an activation window that is based on the log-bell-shaped dose response function which describes the receptor crosslinking involved in the B-cell activation. The rate of activation of B cells does not increase monotonically with the concentration of antigens or anti-idiotypic antibodies (stimulation), as shown in Fig. 1(a). There exists a minimum dose ( $\theta_1$ ) of antigens that will elicit the antibody response, but for a very high antigen dose (greater than  $\theta_2$ ) the response decreases (suppression). In this case two tolerance regions may be defined: low- and high-dose tolerance. In the automata model the stimulus felt by each population (automaton) is defined as a function of the field  $h$  which depends on the concentrations of its anti-idiotypic populations (Weisbuch *et al.*, 1990). The automaton rule is based on the window of activation that reproduces the main features of the dose-response function: the activation ( $\delta_1$ ) and the suppression ( $\delta_2$ ) thresholds [Fig. 1(b)].

The interaction among the antibodies and also the effect of the slightly defective lock-and-keys that is observed in such interactions, are described by using the concept of shape-space (Perelson & Oster, 1979). According to such formalism the shape of a molecule is described by many factors involved in the "pattern recognition" as for instance geometrical shape,

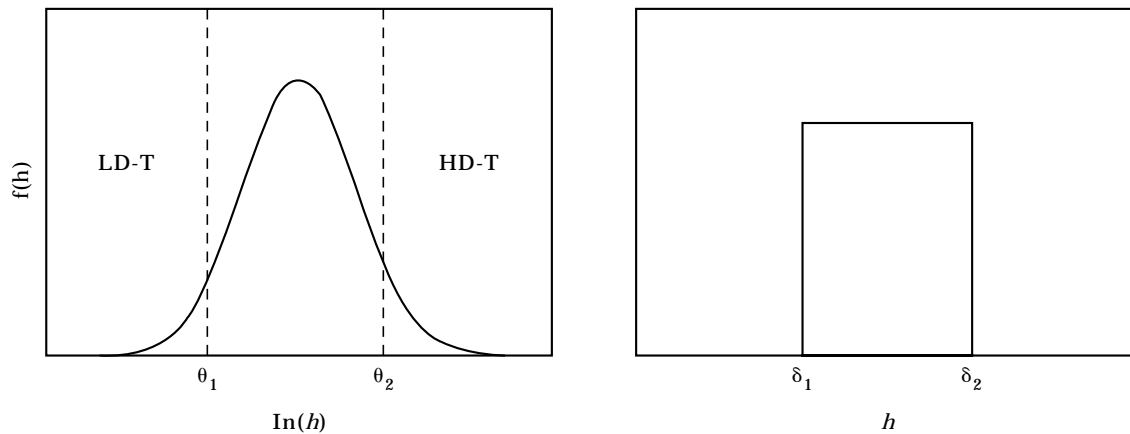


FIG. 1. Schematic representation of the log bell-shaped response function, with the low and high-dose tolerance (LD-T) and HD-T regions defined by the thresholds  $\theta_1$  and  $\theta_2$  (at left) on r.h.s. we present the simplified activation step function used in the cellular automaton rule.

electric charge, hydrophobicity, etc. Hence, in a  $d$ -dimensional space, each dimension is associated with different aspects involved in the B-cell cross-linking. In the original model introduced by De Boer, Segel and Perelson (BSP) (1992), the receptors of the B-cells are characterized by a vector  $\mathbf{r}$  in  $d$ -dimensional real space and are assumed to interact if they have complementary shapes. The interaction is maximal whenever the spatial coordinates are equal and opposite (i.e.,  $\mathbf{r}$  and  $-\mathbf{r}$ ) and decays for less complementary shapes according to a Gaussian function of the Euclidean distance between the pair of interacting shapes. The space is discrete and the concentrations are also assumed to be discrete in a logarithmic scale. By performing simulations in one and two dimensions, they observed that starting from a nearly homogeneous distribution of initial populations of different cells, the final distribution is very inhomogeneous: at some points of the network the cell populations are orders of magnitude above those for other points. In two dimensions these high-population sites tend to cluster in small circles. The concentrations of disconnected activated clones were much smaller (6–8%) than these expected by Coutinho (1989) and Holmberg *et al.* (1989).

As pointed out by Perelson & Oster (1979), if the notion of shape-space is relevant, its dimension should be far larger than 2 (at least  $d \geq 5$ ). In order to study this model in higher dimensions, Stauffer & Weisbuch (1992) introduced a simplified version of the BSP model (BSP III). They replaced the Gaussian distribution of interactions by nearest-neighbour interactions, and the B cell concentrations, which could assume any value in the BSP model, were now restricted to assuming only three values representing the virgin ( $B = 0$ ), suppressed ( $B = 1$ ) and immune ( $B = 2$ ) states. This three-peak structure was obtained

by the authors for the final distribution of concentrations from the original model, just by replacing Gaussian with nearest neighbours interactions. With this simplified version of the BSP model they obtained a transition from stable to chaotic regimes in high dimensions ( $d \geq 4$ ), but for lower dimensions ( $d \leq 3$ ) the system always evolves to stable configurations (fixed points or limit cycles). Nevertheless, the authors pointed out that the chaotic regime, similar to the stable one, would probably not be interesting to describe the dynamics of the immune system. In further work one of us has studied how the system attains this chaotic regime and a possible interpretation for its biological meaning (Zorzenon dos Santos, 1993). The same kind of behaviour (stable-chaotic transition) was also observed in a non-deterministic two-state model (defining only high and low concentration of B-cells) (Stauffer, 1994; Sahimi & Stauffer, 1993).

In recent work, we have shown that the stable-chaotic transition on this model can be obtained even for lower dimensions ( $d \geq 2$ ) (Zorzenon dos Santos & Bernardes, 1995), depending on the activation threshold ( $\delta_1$ ) and the width of the activation interval of the window ( $\delta_2 - \delta_1$ ) defined by the automaton rule. The stable-chaotic transition is obtained until a certain critical value of the activation threshold is attained, above which this transition disappears and the system always evolves towards a stable configuration. The shorter the activation interval the faster the system goes to the chaotic behaviour. Moreover, we have observed that the final results are sensitive to the choice of the initial distribution of concentrations (or states). This kind of stable-chaotic transition has also been observed for the non-deterministic model in lower dimensions, provided that one increases the number

of neighbours that influence each site on the lattice (Meyer, 1995).

From the network theory and some experimental evidence mentioned above, we would expect the behaviour of the repertoire to be described by some sort of mosaic picture (connected clusters of activated sites embedded in a sea of “disconnected” clones). This “mosaic” would change smoothly during the time evolution due to the network interactions, provided no antigen is presented. Under antigen presentation we would expect a more drastic change of this picture. According to this description, the stable and chaotic regimes are not interesting from the immunological point of view. In the stable region, the system always evolves to fixed points or short limit cycles, with almost all  $B$  sites in the virgin state and a low percentage of activated sites, which does not correspond to the dynamical picture of the functional connected network. On the other hand, the chaotic regime, as suggested before, seems to correspond to a non-healthy state, some kind of fully percolated lattice which is of no interest as it will not present self-regulation mechanisms (as for example in the case of septicaemia). Even the very long periods found before attaining the chaotic regime might be interpreted as a long chain of activation, so the system is already trapped in a sort of non-healthy state before attaining the transition region (Zorzenon dos Santos, 1993). However, until now the chaotic regime was not studied in detail to confirm such mechanisms. Although the stable and chaotic regimes do not seem to be interesting from the immunological point of view, the transition region should be investigated, since it could be appropriate to describe the immune repertoire dynamics. From cellular automata studies we have learned that the transition region can exhibit a very complex and interesting behaviour.

The aim of this paper is to investigate whether the BSP III model, using the appropriate window, exhibits the necessary complexity in the transition region to describe the evolution of the immune repertoire according to the network theory proposed by Jerne. As we shall show, it actually does. In the transition region we find a functionally connected network of activated sites embedded in a sea of disconnected clones, exhibiting a dynamical behaviour of aggregation and disaggregation. In this region the model describes the global properties necessary to generate the functional network that will regulate the dynamics of the system and will determine the immune diversity available in the repertoire. The memory comes from the dynamics of the system. We also show that the chaotic regime is of no use in describing immune repertoire evolution.

In Section 2 we describe the model and the results are presented and discussed in Section 3. Finally in Section 4 we present our conclusions.

## 2. The Model

The BSP III model is defined on a hypercubic lattice and, in contrast with other usual lattice models—such as Ising-like ones—a given site is *not* influenced by its geometric neighbours, but by its mirror image and the nearest neighbours of the mirror image. For example, in one dimension, when only one aspect of the generalized receptor shape is taken into account, on a linear chain of  $L$  sites, the site  $i$  does not interact with its nearest neighbours  $i - 1$  and  $i + 1$ , but with the sites  $L + 1 - i$  (the mirror image) and  $L + 2 - i$  and  $L - i$  (the nearest neighbours of the mirror image). The interaction with the neighbours of the mirror image simulates the effect that even a key with minor scratches can still open its lock. In the BSP III model, all interactions have the same strength, in contrast with the original version, where a Gaussian distribution of strengths was assumed. However, as shown by Stauffer & Weisbuch (1992), this simplification does not qualitatively change the final results.

The model is simulated on a  $d$ -dimensional hypercubic lattice (corresponding to  $d$  different aspects of the generalized receptor shape) with  $N = L^d$  sites, in such a way that site  $i$  interacts with  $2d + 1$  sites (centred at its mirror image  $N + 1 - i$ ). The  $N$  sites of the lattice are numbered from  $-N/2 + 1$  to  $N/2$ , going through the system like a typewriter, meaning that periodic helical boundary conditions have been considered. The site variable  $B$  can assume three different values 0, 1 and 2, representing the different immune states (virgin, suppressed and activated or immune). In this paper we use a slightly different version of the BSP III model, since we calculate the field  $h$  in a different way than the one proposed by Stauffer & Weisbuch (1992). Instead of taking into account only the sites with  $B = 2$  influencing the site  $i$ , here we consider the influence of the mirror site and all its neighbours, independent of the state they are, influencing site  $i$ , and therefore the field  $h_i$  is given by:

$$h_i = \sum_j B_{N+1-j} \quad (1)$$

where  $j = i, i \pm 1, i \pm L, i \pm L^2 \dots$ ; the number of terms depending on the dimension  $d$  of the system.

The automaton rule is thus defined as a function of the field  $h$ , and the thresholds of activation and suppression ( $\delta_1$  and  $\delta_2$ , respectively) of the window. If

the field  $h_i$  belongs to the interval  $[\delta_1, \delta_2]$  [see Fig. 1(b)] the variable  $B_i(t+1) = B_i(t) + 1$ , otherwise  $B_i(t+1) = B_i(t) - 1$  (no change is made if it would lead to  $B = -1$  or to  $B = 3$ ). As we have shown in previous work (Zorzenon dos Santos & Bernardes, 1995), the automata behaviour is very sensitive to the window definition, i.e., to the *activation interval* defined by:

$$P_{at} = \frac{(\delta_2 - \delta_1)}{N_c}; \quad (2)$$

and the *activation threshold* defined by:

$$P_1 = \frac{\delta_1}{N_c}, \quad (3)$$

where  $N_c = [2(2d+1) + 1]$  is the number of different possible values of the field  $h$  created by the mirror site and its neighbours. We have also shown (Zorzenon dos Santos & Bernardes, 1995) that the initial configuration of the  $B$  variables may change the final result and therefore some care must be taken in its choice. We should expect that a healthy system will be represented by configurations in which most of the sites are in the  $B = 0$  state, representing the attentive (immunocompetent but resting) cells that will be able to recognize any different foreign molecule presented to the organism (Holmberg *et al.*, 1989; Coutinho, 1989). On the contrary, a majority of  $B = 2$  cells could be interpreted as a highly exposed (to different antigens) system. Though the system is able to recognize  $10^{11}$  different forms, it is not expected that it will recognize such a large number of antigens during its lifetime. Taking the above considerations into account, we started the simulations with a random spatial distribution of  $B$  variables as follows (Zorzenon dos Santos & Bernardes, 1995):  $(1-x)$  of  $B = 0$  and  $\frac{1}{2}x$  of each of  $B = 1$  and  $B = 2$ , where the  $x$  variable defines the initial proportion of virgin, suppressed and immune clones.

All the results presented in this paper are reported as functions of the parameters  $P_{at}$ ,  $P_1$  and  $x$  and they will be mostly focused on the study of the transition region between the stable and chaotic regimes obtained for this automata.

### 3. Results and Discussion

As discussed above, the dynamics in the BSP III model has different types of attractors. For low values of  $x$  the attractors are fixed points or short-period limit cycles (with all or almost all sites having  $B = 0$ ). Increasing the value of the concentration  $x$ , the periods of the limit cycle become longer and longer (Zorzenon dos Santos, 1993) until a stable/chaotic transition is obtained for  $x_c$  (Stauffer & Weisbuch,

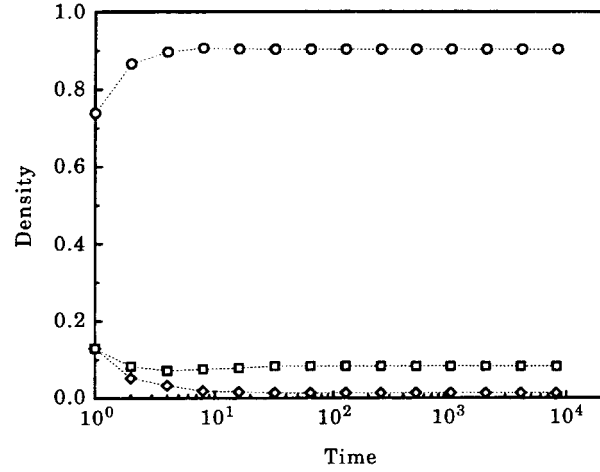


FIG. 2. Time evolution of the densities of sites with  $B = 0$  ( $\circ$ — $\circ$ ), 1 ( $\diamond$ — $\diamond$ ) and 2 ( $\square$ — $\square$ ) for a  $d = 3$  system with  $10^6$  sites, with  $P_1 = 5/15$ ,  $P_{at} = 6/15$  and  $x = 0.26$ . Although a periodic state has not been observed (the system is considered to be in a chaotic regime), the density of  $B = 2$  sites fluctuates around 9%.

1992; Zorzenon dos Santos & Bernardes, 1995) as we will describe below.

Since we mostly study the transition region and the chaotic regime, let us start by analysing the behaviour of the densities of different states in function of time, for concentrations above the critical concentration. In Figs 2 and 3 we plot the percentage of different values of the  $B$  variable on the entire lattice vs. time, for a cubic lattice with  $L = 100$  ( $N =$  number of lattice sites  $= L^d = 10^6$ ), using  $P_1 = 5/15$  and  $P_{at} = 6/15$ , which corresponds to a critical concentration  $x_c = 0.25$ . In Fig. 2 we show the behaviour for  $x = 0.26$ , where in principle an infinite system never reaches a

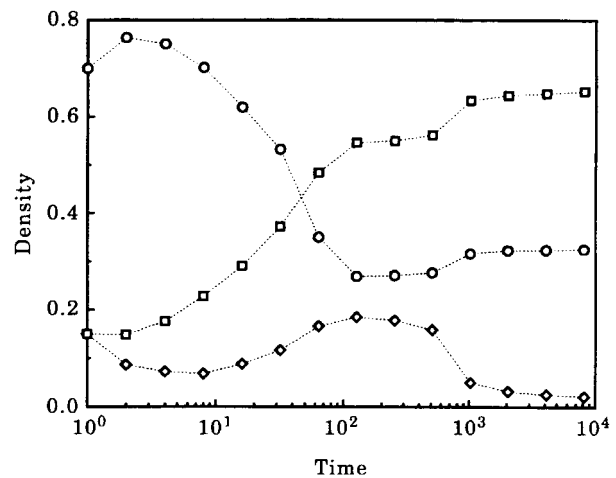


FIG. 3. Time evolution of the densities of sites with  $B = 0$  ( $\circ$ — $\circ$ ), 1 ( $\diamond$ — $\diamond$ ) and 2 ( $\square$ — $\square$ ) for a  $d = 3$  system with  $10^6$  sites, with  $P_1 = 5/15$ ,  $P_{at} = 6/15$  and  $x = 0.30$ . At the end of the simulation (8192 time steps) the system had a majority of the sites with  $B = 2$ .

fixed point or limit cycle (at least for period  $\leq 8192$ ) and fluctuates between different configurations with 90% of the sites with  $B = 0$ , 9% with  $B = 2$  and 1% with  $B = 1$ . In Fig. 3 we show the behaviour for  $x = 0.30$ , where the majority of sites are excited ( $B = 2$ ); in this case, starting from a configuration with most of the sites having  $B = 0$ , the  $B = 2$  sites will form clusters which grow with time, and for  $t > 1000$  those sites will predominate on the lattice, occupying about 65% of the total number of sites. There is a crossover between the behaviours shown in Figs 2 and 3 around  $x = 0.28$ . Above  $x_c$  there are still two different behaviours related to the state of the majority of sites: the first, at the edge of chaos, where most of the sites are in the virgin state which we shall refer to as *transition region*, and the one where most of the sites have  $B = 2$ , from now on referred to as *chaotic region*. Since in the transition region the system always achieves a stationary state (non-periodic) with the majority of sites having  $B = 0$ , it might be possible to find in this region the necessary complex behaviour in order to describe the evolution of the immune repertoire. From the results shown in Fig. 3 we confirm that the chaotic regime is not interesting from the immunological point of view, since most of the sites are activated.

However, the density of different  $B$  variables does not allow us by itself to understand the dynamical behaviour of the system. We need a “local” picture of the system (in terms of the shape space description). In order to get this picture, for each time step we located all the clusters formed by the  $B = 2$  sites and calculated the center of mass of each of those clusters. We have adopted the usual definition of cluster, i.e., if two nearest neighbour sites have  $B = 2$  they belong to the same cluster. Since the lattice sites are numbered from  $-N/2 + 1$  to  $N/2$ , or 1 to  $N$ , the position of each site is defined by only one coordinate and the center of mass of the  $B = 2$  clusters is given by the sum of coordinates of the sites belonging to a given cluster, divided by the number of sites of this cluster. We preferred to adopt this definition of the center of mass, instead of transforming the linear coordinates to  $d$  dimensional space coordinates. Thus, each cluster in the system is defined by its size  $S$  and the center of mass position  $CM$ .

We have performed simulations for different values of parameters in the transition region, and one example of our results is presented in Fig. 4, for a  $d = 3$  lattice with  $L = 46$ ,  $P_1 = P_{at} = 5/15$  and  $x = 0.27$ . The behaviour of the densities of sites, in this case is similar to that described by Fig. 2 and no periodic regime has been found (at least for periods  $\leq 16384$  time steps). After 4100 time steps the number

of  $B = 2$  sites fluctuates around 8000 sites belonging to 1200 different clusters. Although we have obtained data for all time steps, here we present only a short range in the time-scale, in order to avoid overloading the pictures. The lower plot shows the time evolution of the size of the largest cluster  $S_{max}$  found at each time step and the upper plot shows its  $CM$  coordinate. The two plots indicate that for each time step the largest cluster is found in different regions of the lattice. However, the largest cluster changes shape at each time step, thus its evolution is not simply a translation along the lattice. Here we did not find “glider”-structures obtained for some cellular automata [see for example Gallas & Herrmann (1990) and Gallas *et al.* (1992)]. The dynamics of the present system is characterized by local aggregation of small clusters and disaggregation of large ones. If at time  $t$  the largest cluster is found at a certain position, in the next time step  $t + 1$ , a new largest one will be found at another position, which may or may not be in the same region. This means that the largest cluster at time  $t$  can split into small clusters at time  $t + 1$  and/or at time  $t + 1$  a new largest cluster is formed by the aggregation of other clusters. During the time evolution of the system these fission/fusion movements always occur around the same regions of the system, in a non-periodic, but localized movement.

An example of the time evolution of the system configuration is shown in Fig. 5. The coordinates of all sites were converted to three-dimensional coordinates, in order to provide a three-dimensional plot, and only sites with  $B = 2$  are shown. We have chosen three successive time steps, starting at  $t = 4.136$  (the arrows in Fig. 4). In order to get a better illustration of the dynamical evolution described above, only a small portion of the system is shown in Figs 5(a-c) (representing the successive times  $t = 4136, 4137$  and  $4138$  respectively). In such a sequence of pictures, the clusters grow or break or fuse, leading to different cluster sizes at different time steps (see for example the time evolution of the bottom left and upper right corners). However, the center of mass of these different clusters fluctuates around slightly different positions. In Fig. 5(d) we present the entire system configuration at  $t = 4138$ , from which we observe that the  $B = 2$  sites aggregate in many small and different clusters (the inner box represents the portion of the system shown in the previous parts). Thus, the clusters of activated sites (meaning in our model the activated B-cells) are products of the dynamics of the entire system and therefore are not isolated clusters. They interact with other parts of the system, since they oscillate around the same region as a

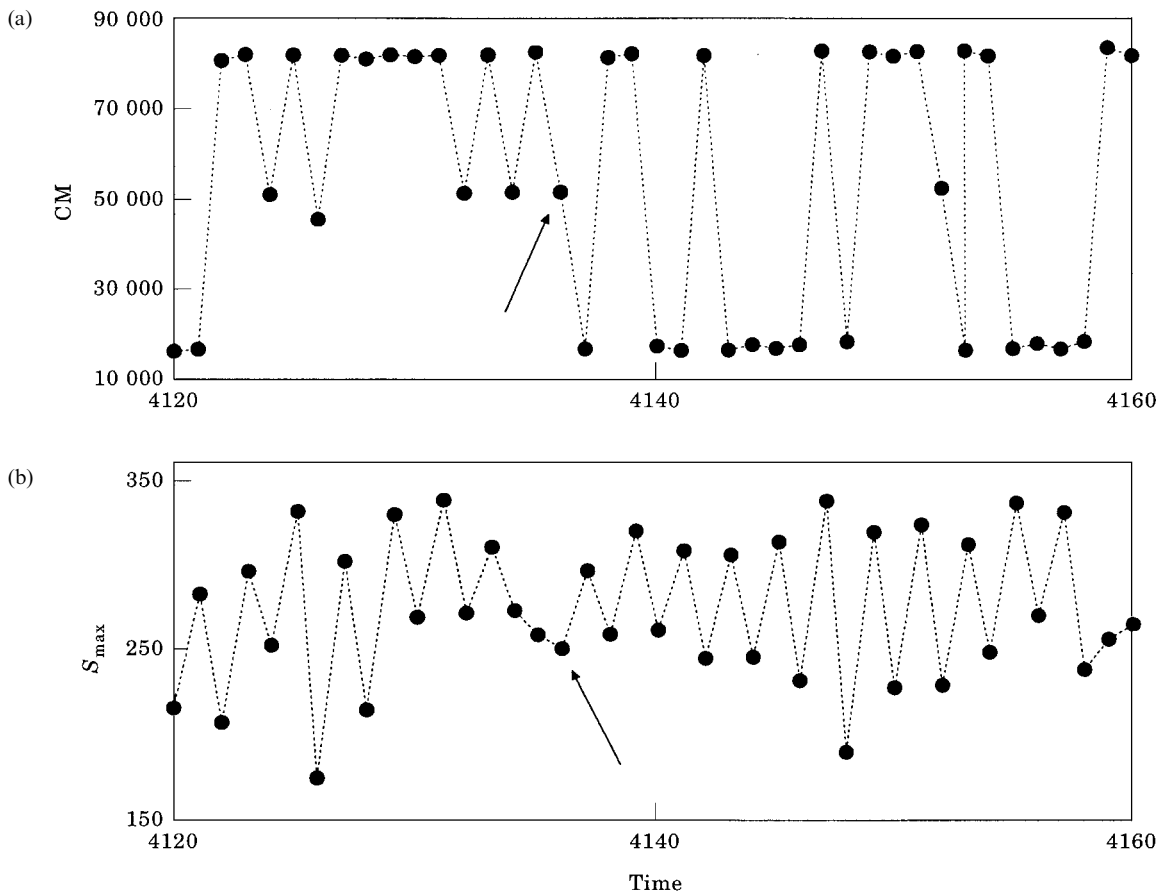


FIG. 4. Time evolution of the largest cluster (only a short period of time is shown): (b) shows the size of the largest cluster  $S_{max}$  and (a) its position  $CM$ . These results were obtained for simulations using  $P_1 = P_{at} = 5/15$  and  $x = 0.27$  for a  $3d$  system with  $L = 46$ . The arrows indicated the values of  $S_{max}$  and  $CM$  at time  $t = 4.136$  (related to the Fig 5).

consequence of the dynamical behaviour of the system.

After having got the picture of the complex behaviour exhibited by this cellular automata in the transition region, let us focus our attention onto two other questions: (1) how does the system respond to a perturbation in the transition region (i.e. how stable is this transition regime)?; (2) Is it possible, using this model, to understand how the memory is generated in the immune system under antigen presentation (which will be represented by the excitation of one small region of the lattice)?

In order to describe a healthy system it is necessary that those perturbations remain finite and localized, in other words, the perturbation is not allowed to percolate through the whole lattice but does not die out either. Following Stauffer & Weisbuch (1992) we used the “damage spreading” approach in order to study the points addressed above [for a general discussion of the theory see Jan & de Arcangelis (1994)]. We have used the standard procedure: first we run a given

sample (say  $C_1$ ) until a previously defined time step  $t_s$  and then the entire system is copied into another one (say  $C_2$ ); after having created the copy we introduce small changes (compared to the size of the system) on the  $C_2$  system. We follow the trajectory of both systems,  $C_1$  and  $C_2$ , and for each time step different quantities are calculated: the Hamming distance  $H_D$  between the systems, the number of clusters that differ between  $C_1$  and  $C_2$ , the center of mass position  $CM_i$  and the size  $S_i$  of those clusters of damage, as well the center of mass position and size of all  $B = 2$  clusters in the  $C_1$  and  $C_2$  systems. The Hamming distance is a measure of the total number of different sites between the systems  $C_1$  and  $C_2$  at a time  $t$  (it does not matter whether they have  $B = 0, 1$  or  $2$ ).

According to Wolfram’s classification of different behaviours of the cellular automata, for class 3, which exhibits a chaotic behaviour, the Hamming distance increases during the time evolution (Wolfram, 1983; Stauffer, 1991); and for class 4, which might exhibit the most complex behaviour and is probably quite

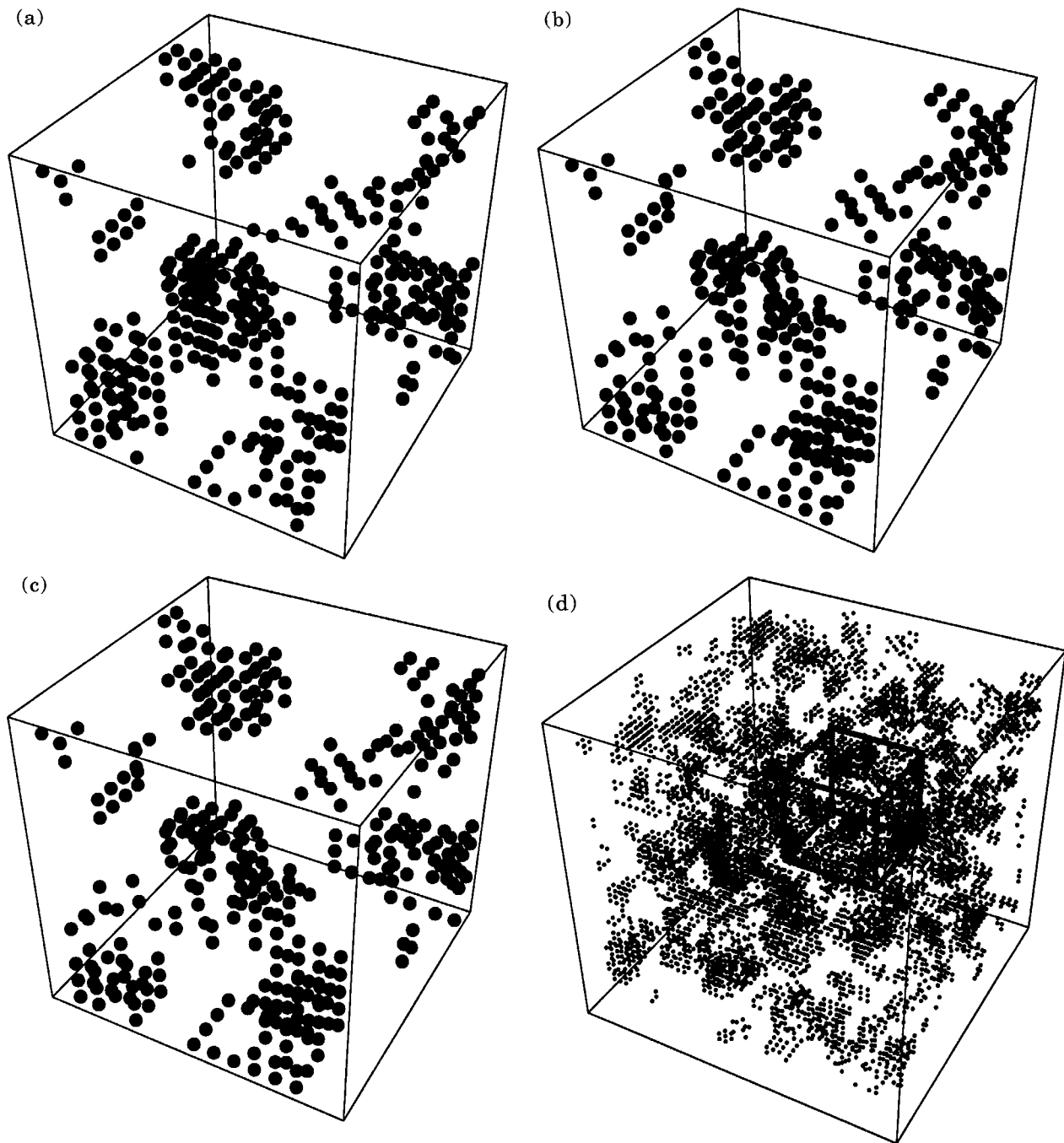


FIG. 5. Three-dimensional plot of the system described in Fig. 4. The linear coordinates of the sites were converted in three-dimensional coordinates and only the sites with  $B = 2$  are shown (filled circles). Figures 5(a–c) show the time evolution of the inner box displayed in Fig. 5(d), at times 4136, 4137 and 4138 respectively. The fission/fusion movement of the clusters (described in the text) can be observed at the bottom left and upper right corners of the successive pictures. The entire system at  $t = 4138$  is shown in Fig. 5(d).

appropriate to model biological systems (Langton, 1986),  $H_D$  fluctuates around a mean value. The conjecture made in a previous paper (Zorzenon dos Santos & Bernardes, 1995) that the BSP III cellular automata seems to exhibit a class 4 behaviour in the transition region, is now supported by the oscillatory behaviour of  $H_D$  around a mean value. We also found

a collective behaviour leading to quasi-periodic structures different, in this case, from the “gliders” observed in other class-4 cellular automata (Gallas & Herrmann, 1990; Gallas *et al.*, 1992). The collective behaviour found on the transition region might have similarities to the collective behaviour observed by Chate & Maneville (1991, 1992), but further

investigation, already in progress, is necessary to better characterize this behaviour.

Damage spreading in this model was first introduced by Stauffer & Weisbuch (1992) by changing the state of all the sites in the middle hyperplane of the lattice. However, we have observed that this procedure can drastically change the behaviour of the system compared to the method we employ below. The reason for this drastic change comes from the fact that, in the transition region the system is characterized by a majority of  $B = 0$  sites, and therefore the change of a whole hyperplane ( $B = 0 \rightarrow B = 2$ ) leads to the instantaneous appearance of a fully-connected cluster of  $B = 2$  sites, which will grow and propagate over the system. In the present work, we define at time  $t_s$  small volumes  $\Gamma_{dam}$  in the shape-space, centered at randomly chosen points  $\mathbf{r}_d$  [those regions are similar to the antigen binding regions defined by Perelson & Oster (1979)]. The choice of a  $\Gamma_{dam}$  volume is done as follows. For a given volume centered at  $\mathbf{r}_d$ , we check out whether all the sites belonging to this volume have  $B = 0$ , as

well as all the nearest-neighbouring sites of this volume, in order to avoid the creation of a  $B = 2$  cluster larger than that previously defined. We also require that the mirror site  $-\mathbf{r}_d$  has  $B = 0$  to ensure that both the  $\Gamma_{dam}$  region and the mirror site  $-\mathbf{r}_d$  are not already excited at  $t_s$ . After selecting those sites, we change their state and that of the mirror sites ( $B = 0 \rightarrow B = 2$ ). The change in the mirror site has been adopted to avoid that at the next time step  $t_s + 1$  the damage is destroyed by statistical fluctuations. However, further simulations showed that the enlargement of the initial damage produces the same results. We follow the evolution of each  $\Gamma_{dam}$  volume introduced, in order to observe whether they are sustained by the dynamics of the system in the regions where they were produced. If the presence of  $B = 2$  clusters continues to be detected in those regions, we calculate the center of mass  $CM_{dam}$  and the sizes of these clusters.

We have performed different simulations for different lattice sizes and dimensions ( $d = 2, 3$  and  $5$ ), always using values for  $x$ ,  $P_1$  and  $P_{at}$  corresponding

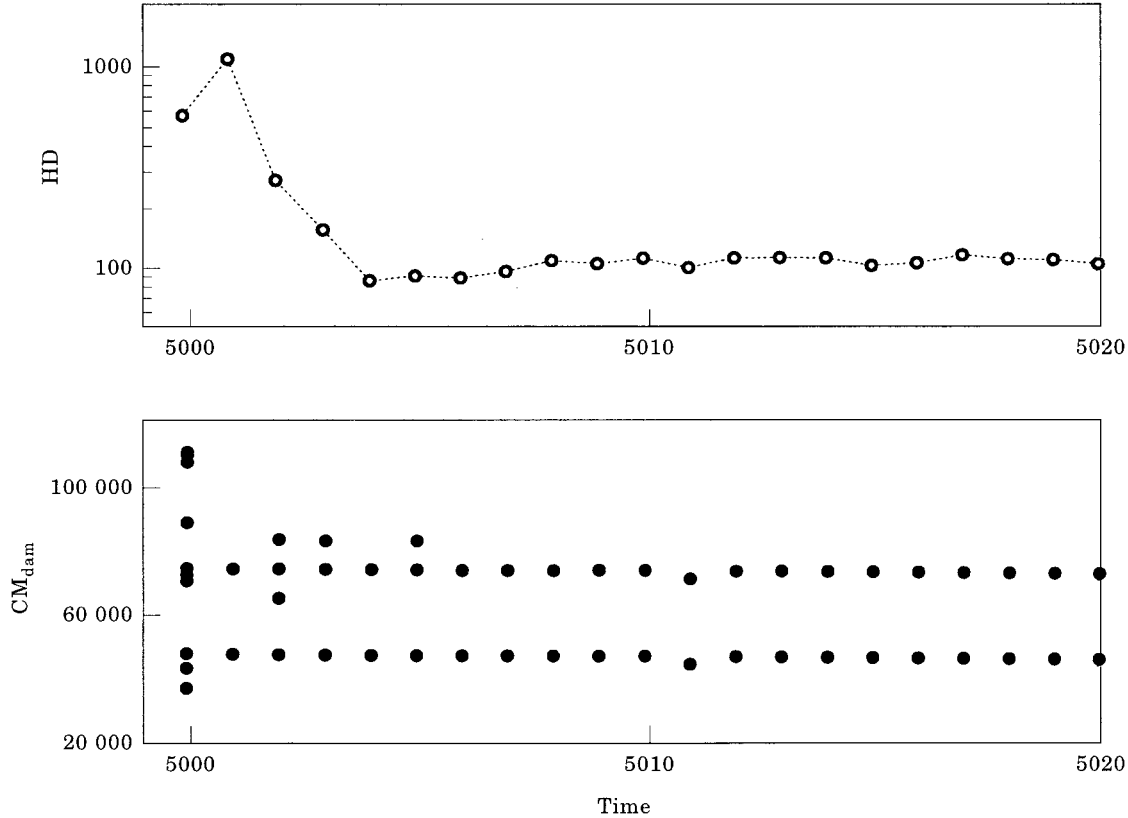


FIG. 6. Results of spreading of damage obtained for a  $d = 3$ ,  $L = 50$  system, for  $x = 0.27$ ,  $P_1 = P_{at} = 5/15$ . At time  $t_s = 5000$  ten clusters of 64 activated sites (including the mirror site) have been introduced in the network. The upper plot shows the time evolution of the Hamming distance  $H_D$  whereas the lower plot shows the evolution of the center of mass of the clusters  $CM_{dam}$  found in the regions where those damages were produce. After six time steps only two of the initial ten clusters survive and their positions stabilize at  $t = 5020$ .

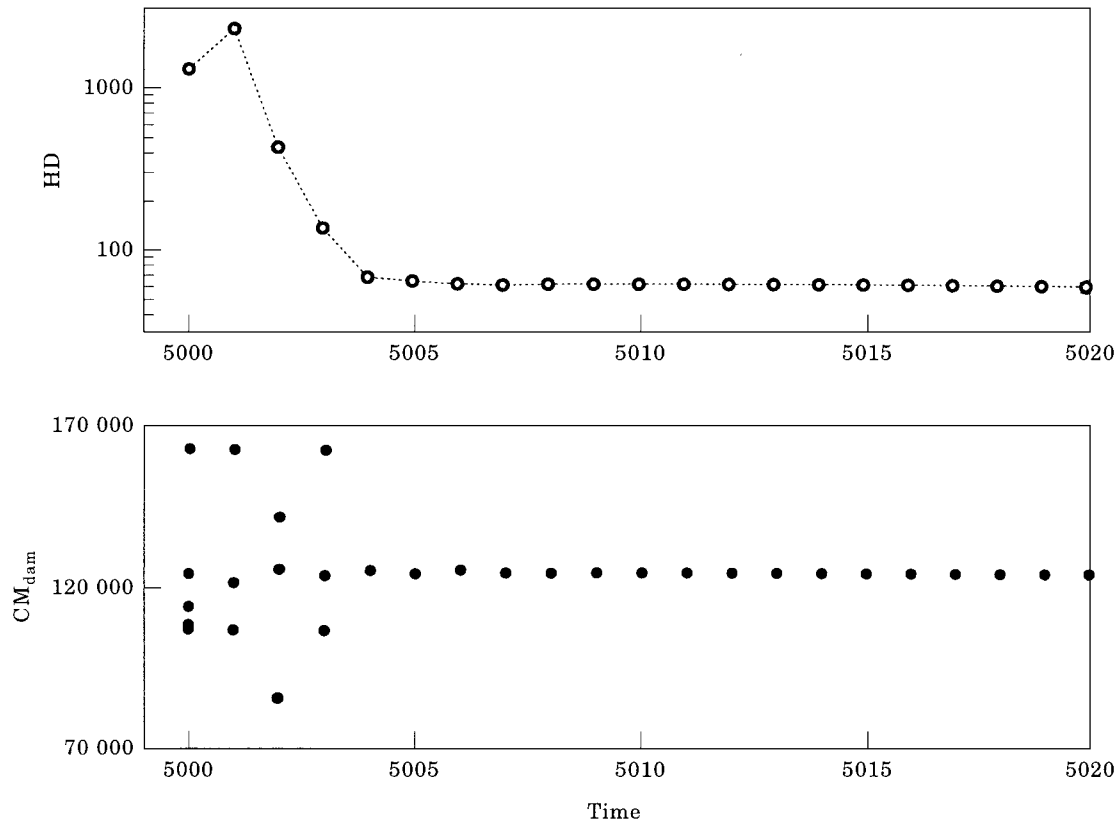


FIG. 7. The same quantities shown in Fig. 6 are shown here for  $d = 5$ ,  $L = 12$  system, for  $x = 0.35$ ,  $P_1 = 8/23$  and  $P_{at} = 7/23$ . Five clusters of 232 activated sites (including the mirror site) have been introduced and only one survived.

to the transition region. The results we present in Figs 6 and 7 were obtained for  $d = 3$  when we introduce ten damages, each of 64 sites and for  $d = 5$  with five damages, each of 232 sites, respectively. In all the simulations a common feature is observed: after the damage is introduced,  $H_D$  increases at the first time step, decays very fast during the next steps and after a few further iterations it fluctuates around a small value (compared with the size of the system), at least one order of magnitude smaller than the initial  $H_D$ . For some of the simulations these fluctuations are periodic, even though we have not detected any periodic behaviour in either of systems  $C_1$  or  $C_2$ , which means that both systems evolve in “parallel” in non-periodic trajectories. In our simulations we did not consider periods greater than 16384. If it is assumed that each time step corresponds to one day, a period of 16384 time steps would represent the order of 44 years, which is longer than the lifetime of the majority of vertebrates.

In Fig. 6 we show the results obtained for  $d = 3$  and  $L = 50$ ,  $x = 0.27$ ,  $P_1 = P_{at} = 5/15$ . The damages were introduced at  $t_s = 5000$ . The lower plot shows the time evolution of the center of mass of the clusters of

damage ( $CM_{dam}$ ) and the upper plot shows the  $H_D$  behaviour during the same period of time. Initially  $H_D$  increases, but after five time steps it decreases and fluctuates around 98, i.e., among the 125000 sites of the two samples only 98 sites are different. Those different sites belong to 16 clusters and only two of them (actually the two largest, with 28 sites each) remain in the regions where the damage was initially produced. The entire  $C_2$  system has around 1500 clusters of  $B = 2$  sites and the largest one has of order of 300 sites. A similar picture was obtained for the  $C_1$  system. In other words, after ten time steps, from the ten damages introduced, only two remained. The center of mass position of each one of the clusters produced by the damage fluctuates and stabilizes around  $t = 5020$ .

The same qualitative behaviour was observed for higher dimensions. Figure 7 shows the results obtained for  $d = 5$ ,  $L = 12$  (248832 sites), using  $P_1 = 8/23$ ,  $P_{at} = 7/23$  and  $x = 0.35$ . In this case we have produced five damages of 232 sites each (meaning an initial  $H_D = 1.160$ ). Again  $H_D$  increases at first, with further decay and finally stabilizes at  $H_D = 56$ , corresponding to nine different clusters

between the two samples  $C_1$  and  $C_2$ , with one large cluster of 48 sites and the other eight clusters of just one site each. The largest cluster remained in the region where one of the damages was introduced.

One piece of evidence for the existence of memory in the immune system comes from the fact that under the first antigen presentation the response will take much longer than the second one due to a second antigen presentation. Moreover, the concentration of antibodies is much higher in the second presentation than in the first one. There are mainly two different explanations for the immune memory: the first one claims the existence of memory cells and the second one considers the memory as a consequence of the dynamics of the system. In the present model, the memory effect should appear as a consequence of the dynamics of the system.

In order to study how the memory is generated in this model we have simulated the first and second antigen presentation. We let the system evolve until a certain time and then introduce the first antigen presentation (the first damage). After 20 time steps ( $t = 5020$ ), when the system has already relaxed, a

second excitation is introduced in the network. Once again, we changed the state of all the sites in the same  $\Gamma_{dam}$  regions chosen at  $t_s$  (if a site already has  $B = 2$ , it remains unchanged). The results for the second antigen presentation are shown in Fig. 8 and were obtained under the same conditions used in Fig. 6. Actually, the results are the same for the time interval [5000, 5020]. As in the first presentation, initially  $H_D$  increases and then decays, fluctuating now around a higher value (200), twice the value obtained after the first presentation. This enhancement of the Hamming distance corresponds to the formation of a new activated cluster (see the lower plot in the figure). After the second presentation, there is a third cluster surviving instead of the only two clusters that “survived” after the first one (Fig. 6). In this case we did not obtain any difference in time and “antibody concentrations” between the first and second antigen presentations. In the BSP III model we are not dealing with concentrations in the sense proposed in the original BSP model. We consider only three different states that represent low, intermediate and high concentrations. Thus, in this case it is impossible to

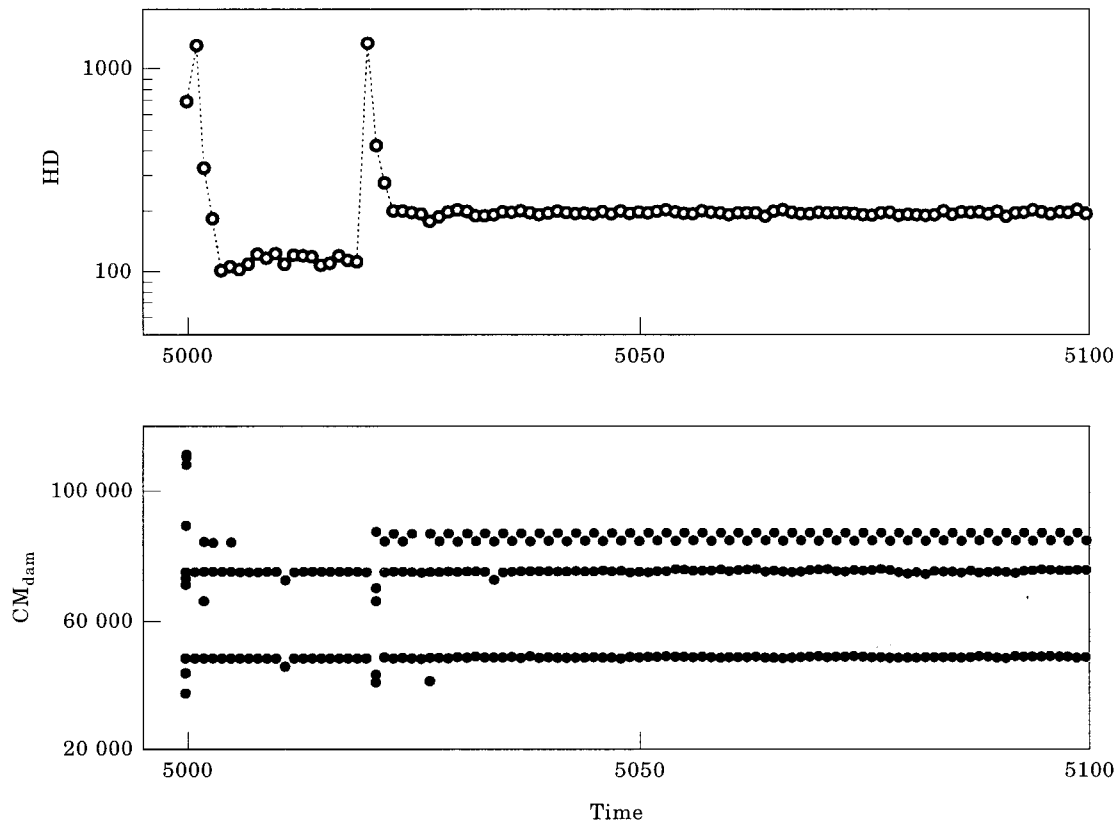


FIG. 8. First and second dose presentation. The quantities discussed in Fig. 6 are now shown for the same system, but now the damages are introduced twice (at different times 5000 and 5020) in the same volumes in shape-space. In contrast with Fig. 6, here a third cluster survived.

reproduce the appropriate variation of the concentrations of a given “antibody”, that would enable us to describe the expected difference between the first and second presentations. Since the time dependence of the response is related to the variation of the antibody concentrations, all the system responses in this model are almost instantaneous.

In Fig. 9 we show the sizes of the five largest clusters among the different ones between  $C_2$  and  $C_1$ , after the first and second presentations. After each presentation large clusters are formed, most of them in the  $\Gamma_{dam}$  regions, corresponding to some sort of expansion of the network until the system relaxes and the distribution becomes almost homogeneous. One possible interpretation for this behaviour is that the network expands aggregating new activated lymphocytes in order to respond and control the damage. Once the situation is under control, the network relaxes incorporating only a few lymphocytes.

In order to better understand the mechanism of memory that comes out from such dynamics, we have performed three antigen presentations under the same conditions used in Figs 6 and 8, but with a different initial configuration, using a different seed of the random number generator. The same ten damages were introduced at  $t = 5000$ , 5150 and 5300 in different regions, as discussed above. The behaviour of  $H_D$  is very similar to that obtained in Figs 6 and 7. After the first presentation it relaxes after a few time steps and fluctuates around 100 sites; after the second one it fluctuates around 200 and finally, after the third presentation the Hamming distance grows to 400 sites. Again, as observed before, the number of remaining clusters increases at each presentation,

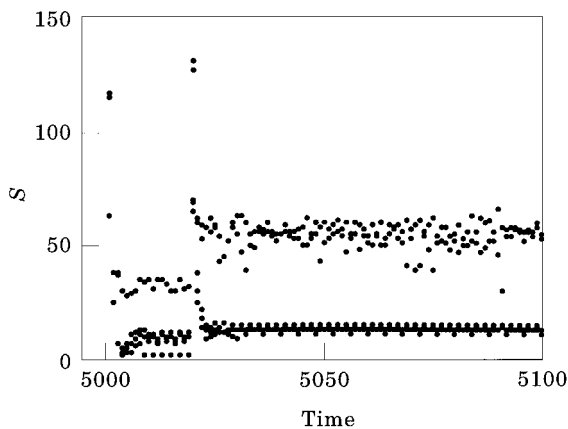


FIG. 9. The time evolution of sizes of the five largest clusters found in the regions where the damages were produced, for the time interval varying from  $t = 500 - 5400$ . The picture includes first (at  $t = 5020$ ) and second (at  $t = 5050$ ) presentations. This distribution corresponds to  $d = 3$ ,  $L = 50$ ,  $P_1 = P_{at} = 5/15$  and  $x = 0.27$ .

some of them appearing in an intermittent way. Moreover, the size of the remaining clusters (which have “survived” in the  $\Gamma_{dam}$  region) also increases after each presentation. In this case, the “immune” memory comes out as an effect of the dynamics of the system leading to an enhancement of the number of activated sites that will belong to the network after each presentation, but still keeping the total number of activated sites that belong to the network small when compared to the total number of sites of the system.

From the results obtained and discussed above, we conclude that this model also reproduces some features of the immune memory under the antigen presentation, due to the fact that activated clusters of  $B = 2$  sites remain in the regions of the shape-space where the damage was produced. However, for the results reported here, some of the damages disappeared after a few time steps and under certain conditions all the damages disappeared after a while. This means that both a specific and a non-specific response [as discussed in the literature, see for example Vaz & Varela (1978), Stewart (1992) and Carvalho *et al.* (1994)] can be modelled by such dynamics.

In Fig. 10 we present the results obtained for three different concentrations above the critical concentration ( $x_c = 0.25$ ) for  $d = 3$ ,  $L = 50$ ,  $P_1 = 5/15$  and  $P_{at} = 6/15$ . In the first and second rows we show the number of  $B = 2$  clusters and the largest cluster size as function of time, respectively. In the third row we present the volumetric fraction  $V_n$  at  $t = 16384$ , which is the number of sites occupied by the clusters of size  $n$  divided by the total number of sites. We have chosen the concentrations  $x = 0.26$ , 0.28 and 0.30. We notice that for  $x = 0.26$  and 0.28 the number of clusters of activated sites oscillates around a mean value at least one order of magnitude greater than the mean value for  $x = 0.30$  (in the chaotic regime). Thus, in the transition region the number of activated clusters is much larger than in the chaotic region. From the results presented in the second row of Fig. 10, we notice that while for  $x = 0.26$  the mean value of  $S_{max}$  is very small compared with the lattice size (the order of  $6/100000$ ), for  $x = 0.28$  this mean value is two orders of magnitude greater ( $1/1000$ ) and for  $x = 0.30$  it corresponds to 65% of the total number of sites. In other words, in the chaotic region we find a huge percolated cluster, which confirms the previous conjectures (Stauffer & Weisbuch, 1992; Zorzenon dos Santos, 1993; Zorzenon dos Santos & Bernardes, 1995), according to which the chaotic region is not interesting from the immunological point of view, since it corresponds to a highly excited non-healthy

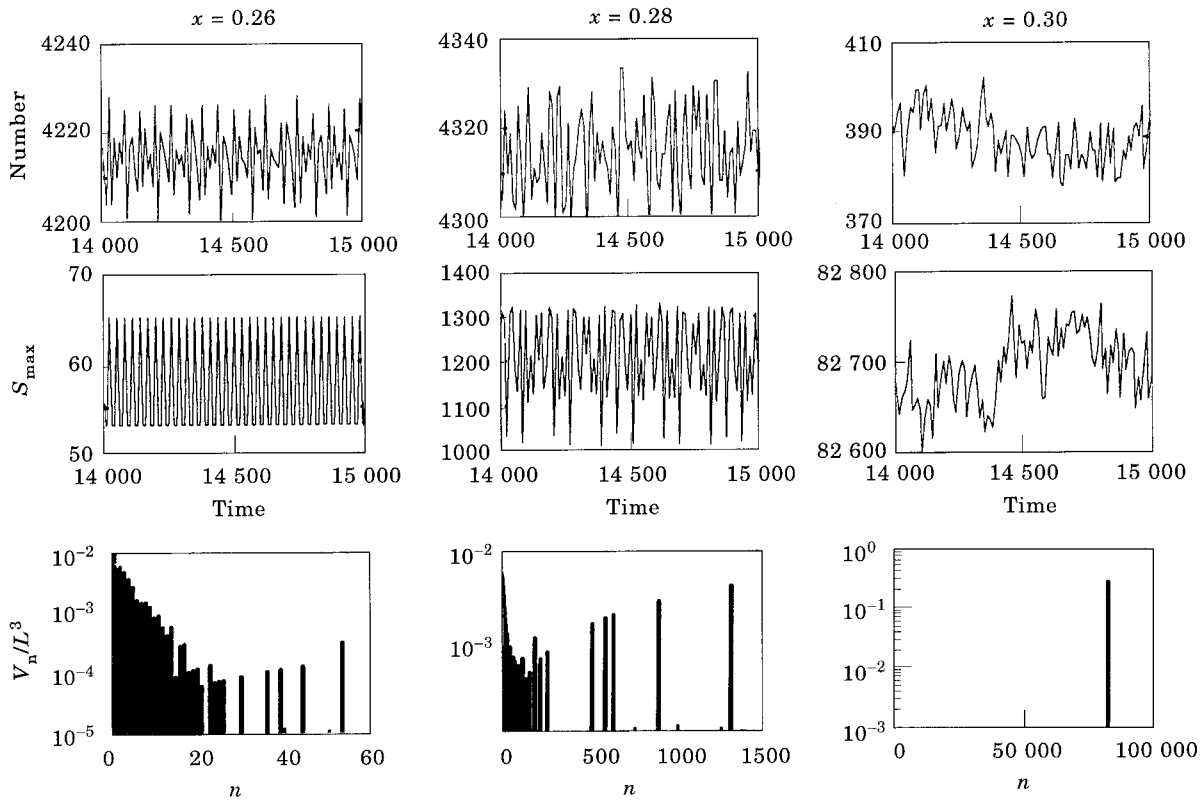


FIG. 10. The results presented in the different columns refer to different concentrations  $x = 0.26, 0.28$  and  $0.30$  above the critical concentration ( $x_c = 0.25$ ), for  $d = 3, L = 50, P_1 = 5/15$  and  $P_{at} = 6/15$ . In the first row we present the variation of number of clusters of activated sites ( $B = 2$ ) during the time interval varying from  $t = 14,000$  to  $15,000$ . In the second row we show the maximum cluster size  $S_{max}$  during the same time interval. In the third row we show the fractional volume with respect to the total volume of the system, of the clusters of size  $n$ .

state. This can be better understood by looking at the pictures of the third row of Fig. 10. While for  $x = 0.26$  and also  $0.28$  the major contributions come from small clusters (in different scales) compared to the size of the system, for  $x = 0.30$  the major contribution comes from a unique huge cluster.

In Fig. 11 we present the temporal evolution of  $H_D$  for  $d = 3, L = 70, P_1 = 5/15$  and  $P_{at} = 6/15$  and  $x = 0.30$ . As expected for the chaotic regime, the HD increases with time.

#### 4. Conclusions

In this paper, by using a simple model we reproduce the kind of dynamics proposed by Jerne to explain the behaviour of the immune repertoire. According to this theory, a finite fraction of the total number of lymphocytes will form a functional network based on the interaction between receptors of complementary shapes, which will regulate the immune response. The lymphocytes that do not participate in this network will form the ensemble of immunocompetent and resting cells that will respond to any foreign antigen; this ensemble will vary from one individual to another, defining the immune repertoire signature. The immune memory will be generated by the dynamics of the network.

The BSP III model consists of simple cellular automata, which can exhibit different kinds of

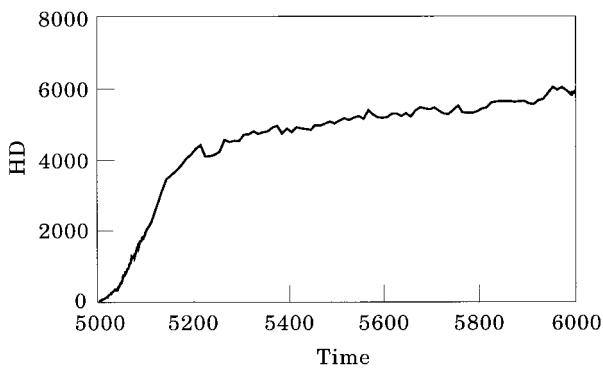


FIG. 11. The time evolution of  $H_D$  for the chaotic region for  $d = 3, L = 50, P_1 = 5/15, P_{at} = 6/15$  and  $x_c = 0.30$ .

dynamics, like stable configuration and chaotic behaviour, which are not suited to describe the immune repertoire evolution. But in the transition region between these two behaviours, corresponding to the edge of chaos, this model exhibits the necessary complexity to describe the dynamical evolution of the immune repertoire according to Jerne's theory. In this region we found the majority of the sites in the virgin state ( $B = 0$ ) while the activated cells ( $B = 2$ ) correspond to 10–20% of the total number of sites and are aggregated in many clusters of different sizes. Those clusters are not disconnected from the entire network, since they are produced by the dynamics of the network itself. At a given time, they might be considered functionally connected. This description of activated clusters embedded in a sea of resting ones corresponds to the proposed mosaic picture of the immune system. During the time evolution, those clusters split or fuse, in some sort of aggregation/disaggregation dynamics always around the same region in shape-space, and the largest cluster is found in different regions. Due to the dynamics of aggregation/disaggregation a new largest cluster is formed at each time step. Then, it is not the same largest cluster that travels around the lattice, as in the case of "glider structures" detected in some class 4 cellular automata. The fluctuation of the size of the activated clusters in the transition region might be interpreted as the oscillatory regime observed in fluctuations of the idiotypes in serum concentrations (Holmberg *et al.*, 1989).

Another important aspect observed in our simulations is that the behaviour of the system is qualitatively the same at low or high dimensions. Perelson & Oster (1979) showed that the biologically relevant dimensionality of the shape-space should be beyond  $d = 4$ , in terms of an effective antigen binding. However, their results were obtained taking into account only the clonal selection hypothesis, without considering the interactions between the lymphocytes, thus there is no network to speak of in their case. Actually, we can find different opinions concerning this matter in the literature, and it seems to be an open question.

We have also investigated how the system responds to the antigen presentation and how the memory is generated by the dynamics of the system. In order to do this, we have worked with the spread of damage approach. In contrast with earlier simulations (Stauffer & Weisbuch, 1992) where a whole hyperplane was changed, we have randomly chosen points in the system and introduced the damages in the regions  $\Gamma_{dam}$  around these points. We have observed that in some cases some of the clusters

created by the damage are sustained by the dynamics of the system, being aggregated to the network. Those clusters, as we have noticed, can be related to the immune memory that is generated in this model. The second antigen presentation (in the same conditions as the first one) produces the enhancement (or survival) of other activated clusters. In other words, after the second dose of antigens new lymphocytes are incorporated to the network. Nevertheless, the number of activated sites still remains around 10–20% of the total number of sites. A third presentation also confirms that the system will always respond to a given antigen in the same way: initially there is an expansion of the number of the clusters of activated sites, but after a few time steps, the system relaxes and will incorporate only few of these new clusters to the network. It should be mentioned that in many cases the activated regions produced by the damage do not survive and vanish. We have not observed any difference in time neither in the antibody concentrations between first and later antigen presentations. Since in the present model we consider only three different states which represent low, intermediate and high concentrations, it is impossible to reproduce the appropriate variation of the concentrations of a given "antibody", that would enable us to describe the expected difference between the first and second presentations. The time dependence of the response is related to the variation of the antibody concentrations and then all system responses in this model are almost instantaneous.

Hence, this model also reproduces some features of the immune memory under the antigen presentation: sometimes, some of the activated clusters remained in the regions of the shape-space where the damage was produced, sustained by the dynamics of the system, sometimes the damages disappeared after few time steps. This means that both a specific and a non-specific response can be modelled.

Of course we know that the solutions of the questions discussed here will not be obtained by computer simulations. However, computer simulations are very flexible and many different scenarios can be explored. For example, if the kind of dynamics described above simulates quite well the theory proposed by Jerne, we may try to learn more about the cooperative and collective behaviour of the immune system by studying such a simple model in more detail. We hope that our results may shed some light on immune research.

We would like to thank D. Stauffer for discussions and suggestions. Computer simulations were performed on several Sun workstations and a DEC-Alpha station at

RRZ, Cologne University. This work is partially supported by the Brazilian Agencies Conselho Nacional para o Desenvolvimento Científico e Tecnológico-CNPq, CAPES and FINEP.

## REFERENCES

- CARVALHO, C. R., VERDOLIN, B. A., DE SOUZA, A. V. & VAZ, N. M. (1994). Indirect effects of oral tolerance in mice. *Scand. J. Immunol.* **39**, 533–538.
- CHATÉ, H. & MANNEVILLE, P. (1991). Evidence of collective behaviour in cellular automata. *Europhys. Lett.* **14**, 409–413.
- CHATÉ, H. & MANNEVILLE, P. (1992). Collective behaviors in spatially extended systems with local interactions and synchronous updating. *Prog. Theor. Phys.* **87**, 1–60.
- COUTINHO, A. (1989). Beyond clonal selection and network. *Immunol. Rev.* **110**, 63–87.
- DE BOER, R. J., SEGEL, L. A. & PERELSON, A. S. (1992). Pattern formation in one- and two-dimensional shape-space models of the immunessystem. *J. theor. Biol.* **155**, 295–333.
- EVANS, S. V., ROSE, D. R., TO, R., YOUNG, M. M. & BUNDLE, D. R. (1994). Exploring the mimicry of polysaccharide antigens by anti-idiotypic antibodies. *J. Mol. Biol.* **241**, 691–705.
- GALLAS, J. A. C. & HERRMANN, H. J. (1990). Investigating an automaton of “class 4”. *Int. J. Mod. Phys. C* **1**, 181–191.
- GALLAS, J. A. C., GRASSBERGER, P., HERRMANN, H. J. & UEBERHOLZ, P. (1992). Noisy collective behaviour in deterministic cellular automata. *Physica A* **180**, 19–41.
- HOLMBERG, D., ANDERSON, A., CARLSSON, L. & FORSGREN, S. (1989). Establishment and functional implications of B-cell connectivity. *Immunol. Rev.* **110**, 84–103.
- JAN, N. & DE ARCANGELIS, L. (1994). Computational aspects of damage spreading. In: *Annual Reviews of Computational Physics I* (Stauffer, D., ed.) pp. 1–16. Singapore: World Scientific.
- JERNE, N. K. (1974). Towards a network theory of the immune system. *Ann. Immuno. (Inst. Pasteur)* **125 C**, 373–389.
- JOHNSON-LÉGER, C. A. & DEAN, C. J. (1994). Presentation of anti-idiotypic antibody is sensitive to ionizing radiation. *J. Immunol.* **153**, 574.
- LANGTON, C. G. (1986). Studying artificial life with cellular automata. In: *Evolution, Games and Learning—Models for Adaptation in Machines and Nature* (Farmer, D., Lapedes, A., Packard, N. & Wendroff, B., eds) Amsterdam: North-Holland.
- MEYER, H. (1995). Simulations of the immunological shape space: influence of the interaction range in an Ising-like model. *Int. J. Mod. Phys. C* **6**, 765–772.
- MONVEL, J. H. B. & MARTIN, O. C. (1995). Memory capacity in large idiotypic networks. *Bull. of Math. Biol.* **57**, 109–136.
- NEUMANN, A. U. & WEISBUCH, G. (1992). Window automata analysis of population dynamics in the immune system. *Bull. Math. Biol.* **54**, 21–44.
- PERELSON, A. S. & OSTER, G. F. (1979). Theoretical Studies of Clonal Selection: Minimal Antibody Repertoire Size and Reability of Self-Non-self Discrimination. *J. theor. Biol.* **81**, 645–670.
- PERELSON, A. S. (1988). *Theoretical Immunology, Parts I & II. SFI Studies in the Science of Complexity*. Redwood City, CA: Addison-Wesley.
- PERELSON, A. S. (1992). Mathematical approaches in immunology. In: *Theory and Control of Dynamical Systems* (Anderson, S., ed.) Singapore: World Scientific.
- SAHIMI, M. & STAUFFER, D. (1993). Ising models above the upper critical dimension: an application to Biology. *Phys. Rev. Lett.* **71**, 4271–4273.
- SCHITTEK, B. & RAJEWSKY, K. (1990). Maintenance of B-cell memory by long-lived cells generated from proliferating precursors.
- STAUFFER, D. (1991). Computer Simulations of Cellular Automata. *J. Phys. A* **24**, 909.
- STAUFFER, D. (1994). Monte Carlo simulation of Ising-like immunological shape space. *Int. J. Mod. Phys C* **5**, 513–518.
- STAUFFER, D. & WEISBUCH, G. (1992). High-dimensional simulation of the shape-space model for the immune system. *Physica A* **180**, 42–52.
- STEWART, J. (1992). Immunoglobulins did not arise in evolution to fight infection. *Immunol. Today* **13**, 396–399.
- STEWART, J. & VARELA, F. J. (1991). Morphogenesis in shape-space. Elementary meta-dynamics in a model of the immune network. *J. theor. Biol.* **153**, 477–498.
- SULZER, B., VAN HEMMEN, J. L. & BEHN, U. (1994). Central immune system, the self and autoimmunity. *Bull. of Math. Biol.* **56**, 1009–1040.
- VAZ, N. M. & VARELA, F. J. (1978). Self and Non-sense: an organism-centered approach to immunology. *Med. Hypot.* **4**, 231–267.
- WEISBUCH, G., DE BOER, R. J. & PERELSON, A. S. (1990). Localized Memories in Idiotypic Networks. *J. theor. Biol.* **146**, 483–499.
- WEISBUCH, G., ZORZENON DOS SANTOS, R. M. & NEUMANN, A. (1993). Tolerance to hormones and receptors in an idiotypic network model. *J. theor. Biol.* **163**, 237–253.
- WOLFRAM, S. (1983). Statistical mechanics of cellular automata. *Rev. Mod. Phys.* **55**, 601–644.
- ZORZENON DOS SANTOS, R. M. (1993). Transient times and periods in a high dimensional shape-space model for immune system. *Physica A* **196**, 12–20.
- ZORZENON DOS SANTOS, R. M. & BERNARDES, A. T. (1995). The stable-chaotic transition on cellular automata used to model the immune repertoire. *Physica A* **219**, 1–12.